Molecular Therapy
Methods & Clinical Development
Original Article

Human iPSC-Derived Neural Crest Stem Cells Exhibit Low Immunogenicity

Vera J. Mehler,[1,2] Chris J. Burns,[1] Hans Stauss,[2] Robert J. Francis,[3] and Melanie L. Moore[1]

[1]Endocrinology Section, Biotherapeutics, National Institute for Biological Standards and Control (NIBSC), Blanche Lane, Potters Bar EN6 3QG, UK; [2]Division of Infection and Immunity, University College London, Gower Street, London WC1E 6BT, UK; [3]Biological Imaging Group, Analytical and Biological Sciences, NIBSC, Blanche Lane, Potters Bar EN6 3QG, UK

Recent clinical trials are evaluating induced pluripotent stem cells (iPSCs) as a cellular therapy in the field of regenerative medicine. The widespread clinical utility of iPSCs is expected to be realized using allogeneic cells that have undergone thorough safety evaluations, including assessment of their immunogenicity. IPSC-derived neural crest stem cells (NCSCs) have significant potential in regenerative medicine; however, their application in cellular therapy has not been widely studied to date, and no reports on their potential immunogenicity have been published so far. In this study, we have assessed the expression of immune-related antigens in iPSC-NCSCs, including human leukocyte antigen (HLA) class I and II and co-stimulatory molecules. To investigate functional immunogenicity, we used iPSC-NCSCs as stimulator cells in a one-way mixed lymphocyte reaction. In these experiments, iPSC-NCSCs did not stimulate detectable proliferation of $CD3^+$ and $CD3^+CD8^+$ T cells or induce cytokine production. We show that this was not a result of any immunosuppressive features of iPSC-NCSCs, but rather more consistent with their non-immunogenic molecular phenotype. These results are encouraging for the potential future use of iPSC-NCSCs as a cellular therapy.

INTRODUCTION

Induced pluripotent stem cells (iPSCs) hold great promise in regenerative medicine because of their ability to self-renew and differentiate into any cell type from the three germ layers. Key to the acceptance of iPSCs as a viable therapeutic option is the requirement to demonstrate that these cells are safe for clinical use. One of the key considerations is the immune response of the recipient to the engrafted cells. Although autologous iPSC derivatives should, theoretically, be readily immune tolerated by the recipient, the prohibitive cost and time required for this approach[1,2] means that the clinical utility of iPSCs is expected to be based on allogeneic starting materials. This is the case for several current clinical trials.[3,4] One issue with this approach is the inherent risk of any allogeneic transplant, that of immune rejection of the grafted cells by the recipient. Several reports have suggested that iPSC-derived cells, including iPSC-derived neural stem cells,[5] iPSC-derived dendritic cells (DCs),[6] and iPSC-derived cartilage,[7] exhibit low immunogenicity *in vitro*. Moreover, it has been proposed that iPSCs[8] and iPSC-derived neural stem/progenitor cells are immunosuppressive.[5] On the other hand, studies investigating the immune profile of iPSC-derived cardiomyocytes and smooth muscle cells (SMCs) suggest that they are immunogenic,[9–11] consistent with their status as immunologically mismatched cells. These contrasting reports regarding the immunogenic potential of iPSC derivatives may be explained by differential immunogenicity between different cell types. Indeed, studies that compared different cell phenotypes, differentiated from the same iPSC line, support this hypothesis of differential immunogenicity.[10–12] As a result, it will be essential to systematically characterize the immunological phenotype of the specific iPSC-derived cell type prior to clinical application.

IPSC-derived neural crest stem cells (iPSC-NCSCs) have promising application in regenerative medicine. The neural crest is a transient embryonic cell population that arises during vertebrate development and gives rise to a wide range of cell types, including melanocytes, peripheral neurons, smooth muscle, bone, cartilage, and fat cells.[13] Although the application of NCSCs in regenerative medicine has yet to be widely reported, their broad differentiation capacity means they have the potential to be used as a cellular therapy in conditions such as peripheral nerve injuries, corneal blindness, tooth regeneration, pathological melanogenesis, Hirschsprung disease, and cardiac repair and regeneration (reviewed in Zhu et al.[14] and Achilleos and Trainor[15]). However, the potential immunogenicity of iPSC-NCSCs has yet to be explored. Although it is possible to isolate low numbers of NCSCs from adult tissue, they display a more restricted differentiation and self-renewal capacity compared with their embryonic counterparts.[15] Due to the transient embryonic nature and limited availability of adult NCSCs, pluripotent stem cells represent an exciting alternative source for NCSC generation. Indeed, NCSCs

Received 2 October 2019; accepted 28 December 2019;
https://doi.org/10.1016/j.omtm.2019.12.015.

Correspondence: Vera J. Mehler, Endocrinology Section, Biotherapeutics, National Institute for Biological Standards and Control (NIBSC), Blanche Lane, Potters Bar EN6 3QG, UK.
E-mail: vera-mehler@t-online.de

have already successfully been differentiated from embryonic stem cells (ESCs)[16] and iPSCs.[13,17] Moreover, in a rat model of sciatic nerve gaps, transplanted iPSC-NCSCs have been shown to promote axonal myelination, differentiate into Schwann cells, and integrate into the myelin sheath around axons.[18] In another study, using mice with an early defect of the enteric neural crest resulting in an aganglionic phenotype of the gut, NCSCs colonized the aganglionic embryonic gut and differentiated into putative enteric neurons.[16] There is also evidence that iPSC-NCSCs can stimulate endogenous regeneration of tendon tissue in a rat tendon window defect model.[19] If the potential of NCSCs in regenerative medicine is to be realized in the future, a characterization of the immune profile of these cells will be an important determinant of their clinical safety. Here, we show that iPSC-NCSCs exhibit negligible immunogenicity on a molecular and functional level, suggesting their potential utility in clinical application.

RESULTS

Directed Differentiation of iPSCs Yields HNK-1$^+$p75^{high} NCSCs

We generated NCSCs from two different iPSC lines (NIBSC8 and NIBSC35) in order to assess their immunogenic potential *in vitro*. NCSC differentiation from iPSCs was achieved following a previously published method.[17] Over this 7-day differentiation protocol (outlined in Figure 1A), the cells changed morphologically from colony-forming pluripotent iPSCs to stellate-like putative NCSCs (Figure 1B). Expression of the surface markers HNK-1 and p75 (herein termed HNK-1$^+$p75^{high}) is used to identify putative NCSCs in accordance with previously published reports.[17,20] Somatic NCSCs are not easily accessible due to their transient embryonic nature, and so we validated the differentiation protocol by comparing the yield of HNK-1$^+$p75^{high}-expressing cells from iPSCs to putative NCSCs derived from H9 ESCs. H9 ESCs have been shown to be a viable starting population for NCSC differentiation.[16,17] Here, H9 ESCs and NIBSC8 and NIBSC35 iPSCs gave rise to comparable levels (% of total cell population) of HNK-1$^+$p75^{high} NCSCs (H9: 55.6%; NIBSC8: 52.8%; NIBSC35: 57.1%) after directed differentiation toward a neural crest fate (Figure 1D). In addition, characterization of gene expression levels of key NCSC markers, including *AP2*, *SOX9*, *p75*, and *PAX3*, showed upregulation of these markers in iPSC-NCSCs compared with their pluripotent counterpart. Moreover, neural crest differentiation was accompanied by a downregulation of pluripotency genes relative to the undifferentiated control (Figure 1C). Beyond the molecular phenotype, functional analysis of iPSC-NCSCs was performed by assessing their differentiation capacity. Both iPSC-NCSC populations gave rise to peripheral neurons and mesenchymal stromal cells (MSCs) after directed differentiation and/or spontaneous differentiation (Figures S1 and S2), suggesting the generation of cells with a functional neural crest phenotype.

iPSC-NCSCs Lack Basal Expression of HLA and Costimulatory Molecules

To characterize the immune profile of iPSC-NCSCs, we analyzed the expression of human leukocyte antigen (HLA) and co-stimulatory molecules. Because interferon (IFN)-γ and/or tumor necrosis factor (TNF)-α are known to induce expression of immune-related antigens, the expression of HLA class I and class II molecules, CD40, CD80, and CD86, was assessed without cytokine treatment (untreated) and after exposure to IFN-γ and/or TNF-α treatment (Figure 2A). For the purposes of comparison, the expression levels of immune-related antigens in iPSC-NCSCs (NIBSC8 and NIBSC35) were compared with the expression in a range of other cell types, including DCs, undifferentiated iPSCs (NIBSC8), and iPSC-derived SMCs (Figure 2B). DCs constitutively express both HLA and costimulatory molecules and were included here as a positive control. SMCs derived from iPSCs have previously been shown to be immunogenic[10,21] and genetic modification, resulting in lack of MHC class I and class II expression that contributes to hypoimmunogenicity of these cells.[21] Pluripotent stem cells, including iPSCs and ESCs, have been shown to express low levels of MHC class I molecules, but not to express MHC class II.[6,22] DCs were derived from monocytes (Figure S3), and SMCs were differentiated from NIBSC8, the same iPSC line that served as a starting population for NCSC generation (Figure S4).

At basal level (untreated) and after TNF-α treatment, iPSC-NCSCs showed low expression of HLA class I, with the percentage between 2%–13% (untreated) and 12%–28% (after TNF-α) of HLA class I-positive cells similar to that of undifferentiated iPSCs. This is significantly lower than the percentage of HLA class I-positive cells in iPSC-SMCs (72.47% ± 2.36%). As expected, IFN-γ induces expression of HLA class I in undifferentiated iPSCs (54.43% ± 2.39%) in line with previous reports[6,22] and also in both iPSC-NCSC cell populations (99.23% ± 0.20% and 98.93% ± 0.12%) and iPSC-SMCs (99.87% ± 0.03%). Compared with basal expression in DCs, low levels of HLA class II-, CD80-, and CD86-positive cells were seen in undifferentiated iPSCs and all derivatives both basally and after individual cytokine treatment. Although the percentage of cells expressing CD80 and CD86 was increased in both iPSC-NCSC lines after dual IFN-γ + TNF-α treatment to a statistically significant level in comparison with undifferentiated iPSCs and iPSC-SMCs, this was still markedly lower than the percentage of CD80- and CD86-positive cells seen in DCs. CD40 expression was also low in untreated iPSC-NCSCs and after IFN-γ treatment, whereas the percentage of CD40-positive cells in iPSC-SMCs was significantly increased after IFN-γ treatment (40.73% ± 1.51% in iPSC-SMCs versus 5.25% ± 0.26% in NIBSC8-NCSCs; $p < 0.0001$). Combined exposure to IFN-γ + TNF-α induced an increase in the percentage of cells expressing CD40 in iPSC-NCSCs above basal level, but this remained significantly lower than that observed in iPSC-SMCs.

Taken together, these data reveal low levels of immune-related antigen expression in all iPSC-NCSCs under basal conditions. This would suggest that, in a non-inflammatory environment, iPSC-NCSCs exhibit low immunogenicity, with low antigen-presenting function. To further investigate the immune profile of iPSC-NCSCs, we next assessed their immunogenicity on a functional level.

iPSC-NCSCs Fail to Stimulate Lymphocytes

A one-way mixed lymphocyte reaction (MLR) was used to assess T cell proliferation in response to iPSC-NCSCs and iPSC-SMCs.

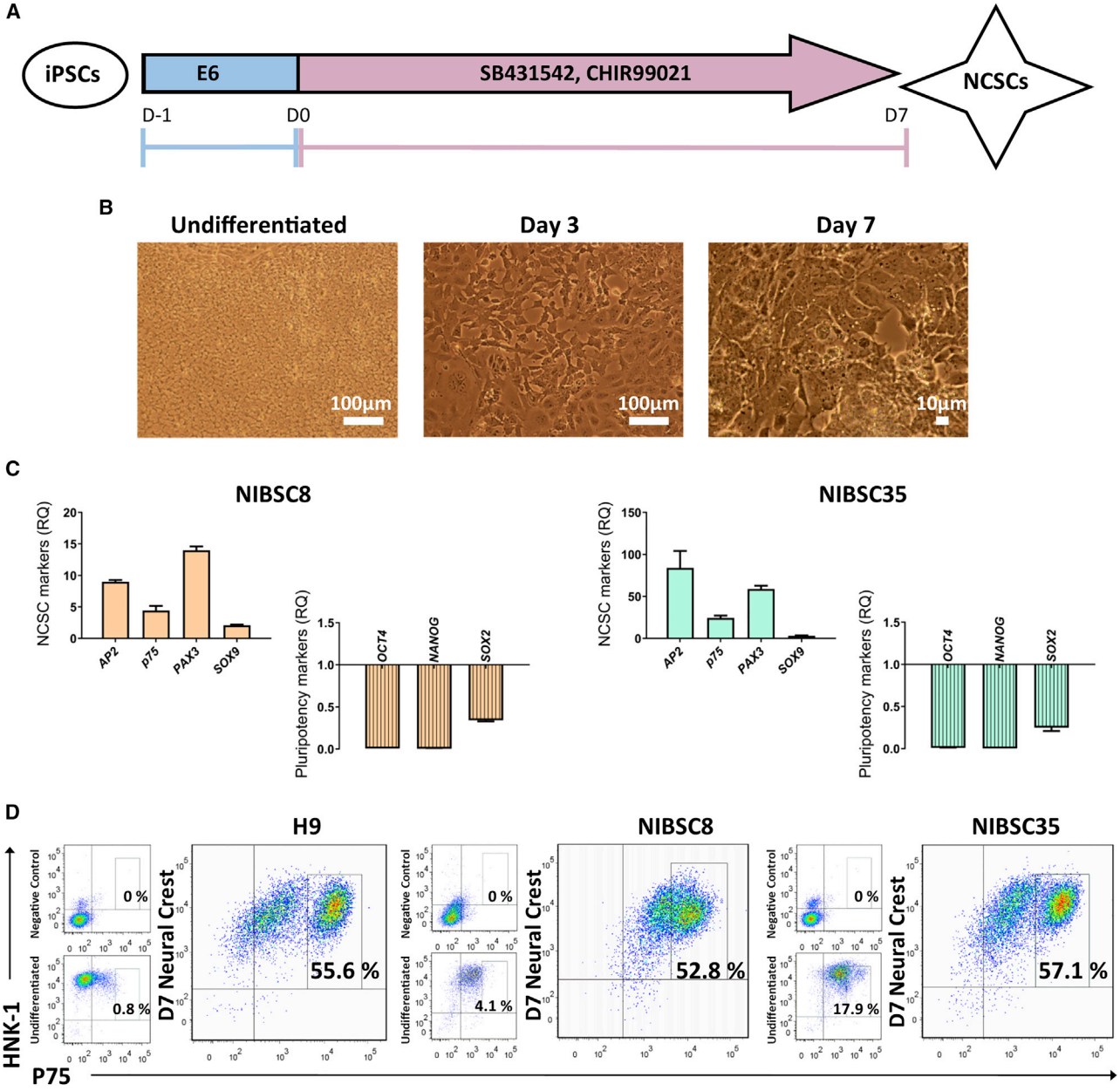

Figure 1. Characterization of iPSC-Derived NCSCs

(A) Schematic outline of directed differentiation toward neural crest lineage. Reproduced from Hackland et al.[17] (B) Representative bright-field images of NIBSC8 iPSCs at days 0 (pluripotent), 3, and 7 of NCSC differentiation. (C) qPCR data from day 7 differentiated iPSC-NCSCs for expression of key NCSC and pluripotency genes. The fold change in expression relative to the day 0 pluripotent control is shown (relative quantification [RQ]). n = 3 biological replicates per line; error bars represent ± SEM. (D) The NCSC markers HNK-1 and p75 were detected by flow cytometry for undifferentiated pluripotent H9 ESCs, NIBSC8 and NIBSC35 iPSCs, and NCSCs (after 7 days of differentiation) and compared with an isotype control (negative control).

Levels of proliferation after co-culture were determined by quantifying Ki-67^{+} cells (Figure 3A) and numerically expressed as stimulation index (SI), representing proliferative cells relative to an autologous control. A response was considered positive when the SI was $\geq$2.[23,24] Immunogenicity of iPSC derivatives was determined with mismatched peripheral blood mononuclear cells (PBMCs) in the MLRs (HLA typing data are provided in Table S1).

Both iPSC-NCSC lines triggered negligible levels of total CD3^{+} T cell proliferation (SI was 0.88 ± 0.05 for NIBSC8-NCSCs and 1.163 ± 0.07

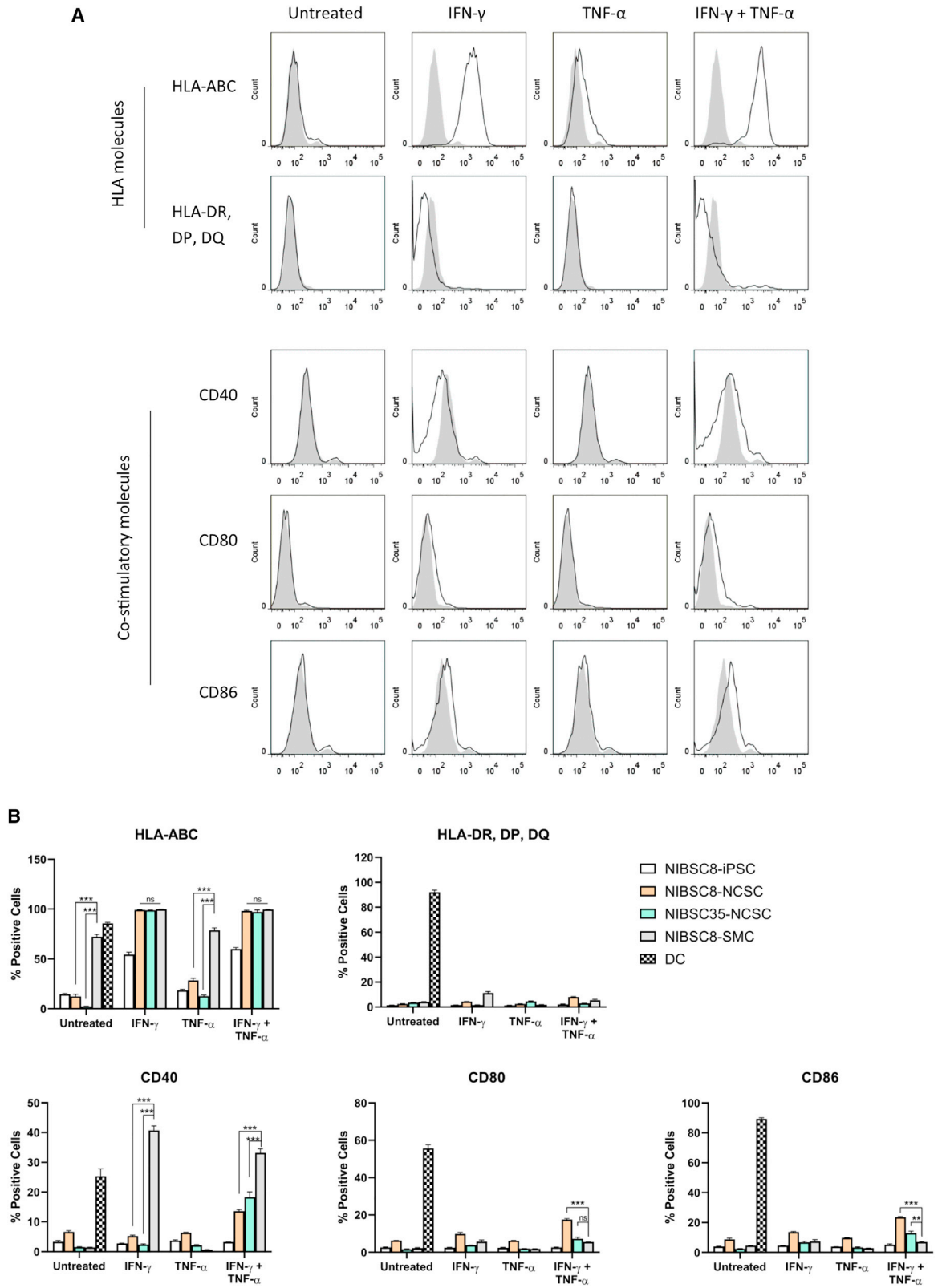

(legend on next page)

for NIBSC35-NCSCs). In contrast, both iPSC-derived SMCs and the allogeneic control (allo-PBMC) significantly stimulated total $CD3^+$ T cell proliferation (2.57 ± 0.50 and 2.16 ± 0.29, respectively). A more striking difference in proliferation response was observed when analyzing $CD3^+CD8^+$ T cell proliferation ($CD3^+CD4^+$ T cells showed a very similar pattern of proliferation to total $CD3^+$ T cell and therefore data are not shown). IPSC-NCSCs did not induce $CD3^+CD8^+$ T cell proliferation above baseline levels (SI was 0.92 ± 0.09 for NIBSC8-NCSCs and 1.09 ± 0.07 for NIBSC35-NCSCs), and this was in stark contrast with iPSC-SMCs, which stimulated significant proliferation of $CD3^+CD8^+$ T cells (9.723 ± 3.43).

Next, we assessed the production of pro-inflammatory cytokines as an additional measure of the stimulation of an immune response. To determine whether the inability of iPSC-NCSCs to stimulate T cell proliferation correlates with the secreted cytokine milieu, we assessed concentrations of IFN-γ, interleukin-1β (IL-1β), IL-2, IL-6, IL-10, IL-12-p70, and TNF-α from the MLRs using multiplex immunoassays. Cytokine production stimulated by autologous (auto) PBMCs is defined as the baseline level.

Corresponding with increases in T cell proliferation, iPSC-derived SMCs and allogeneic PBMCs induced proinflammatory cytokine production, whereas iPSC-NCSCs did not. Notably, the induction of cytokines characteristic of a pro-inflammatory "type 1" T cell response was significantly elevated in response to allo-PBMCs (16-fold higher than auto-PBMCs) and to a lesser extent by iPSC-SMCs (5-fold higher than auto-PBMCs). Conversely, iPSC-NCSCs did not induce IFN-γ levels higher than basal level ($p > 0.9999$). Similarly, TNF-α production was induced by allo-PBMCs (2.5-fold higher than baseline, $p < 0.0001$), but not by iPSC-NCSCs. In addition, the levels of IL-1β, IL-2, IL-6, and IL-12p70 were also not upregulated in response to iPSC-NCSCs, but were significantly increased in co-cultures with iPSC-SMCs (IL-1β: 58-fold, $p < 0.0001$; IL-2: 3-fold, $p < 0.0001$; IL-6: 66-fold, $p < 0.0001$). Interestingly, IL-10 release was also not induced by iPSC-NCSCs. The production of IL-10 has previously been associated with an immunosuppressive phenotype of iPSCs.[22]

Low Immunogenicity of iPSC-NCSCs Is Not a Result of Immunosuppression

To further investigate whether the lack of immunogenicity of iPSC-NCSCs may be explained by an immunosuppressive phenotype, we assessed whether iPSC-NCSCs can suppress the proliferation of highly activated T cells. To test this, we co-cultured iPSC-NCSCs with anti-CD3/anti-CD28-stimulated PBMCs and measured the reduction in T cell proliferation. This reduction was represented by carboxyfluorescein succinimidyl ester $(CFSE)^{low}$ cells (see Figure 4B) and was expressed relative to stimulated PBMCs only. Bone marrow-derived mesenchymal stromal cells (BM-MSCs) are known to be immunosuppressive,[25–27] with some evidence suggesting the same is true for MSCs derived from iPSCs.[28,29] In line with this, we used BM-MSCs as a positive control and generated MSCs from the same iPSC line that was used for NCSC differentiation (NIBSC8). Co-cultures were maintained without a transwell system (w/o tw) and within a transwell system (tw), which allowed the assessment of whether any immunosuppression was mediated by the exchange of soluble factors only (see Figure 4A).

As expected, BM-MSCs significantly suppressed total $CD3^+$ T cell proliferation (0.31 ± 0.03, $p < 0.0001$) and $CD3^+CD8^+$ T cell proliferation (0.52 ± 0.08, $p = 0.0008$) in both assay formats (see Figure 4C). Similarly, iPSC-MSCs reduced total $CD3^+$ T cell proliferation (0.61 ± 0.04, $p < 0.0022$ tw; 0.51 ± 0.05, $p < 0.0001$ w/o tw) and $CD3^+CD8^+$ T cell proliferation (0.56 ± 0.03, $p < 0.0001$ tw; 0.72 ± 0.11, $p = 0.1366$ w/o tw). In contrast, iPSC-NCSCs did not cause a reduction in proliferation of total $CD3^+$ T cells (0.90 ± 0.08, $p > 0.999$ w/o tw; 0.85 ± 0.09, $p = 0.6447$ with tw) or in $CD3^+CD8^+$ T cell proliferation (0.92 ± 0.10, $p > 0.999$ w/o tw; 0.98 ± 0.06, $p > 0.999$ with tw), suggesting that NCSCs do not exhibit a suppressive phenotype and that the low immunogenicity of iPSC-NCSCs is not a result of immunosuppression.

DISCUSSION

NCSCs hold great potential in regenerative medicine;[14,15] however, due to their restricted availability, studies exploring that potential have remained few, and their application in regenerative medicine has so far been evaluated only in animal models.[16,18,19] In this study, we have evaluated the likely immunogenicity of NCSCs. We have differentiated NCSCs from two different iPSC lines, NIBSC8 and NIBSC35. The iPSC lines were generated using different initial cell types and using different reprogramming strategies, accounting for potential differences in immunogenicity that could have been caused by an epigenetic signature inherited from the somatic cell type or off-target effects caused by the reprogramming process. Both iPSC lines were differentiated into $HNK\text{-}1^+p75^{high}$ NCSCs, which were accompanied by upregulation of NCSC marker expression, including *AP2*, *SOX9*, *p75*, and *PAX3*. Although presence of the above markers has been associated with NCSC identity, the determination of specific NCSC markers has proved challenging because NCSCs are a somewhat transient and heterogeneous cell population.[30] In line with this, our data also suggest that the differentiated NCSCs are composed of cell populations exhibiting some heterogeneity. This becomes apparent when considering the percentage of $HNK\text{-}1^+p75^{high}$ NCSCs after directed differentiation, which represent a distinct population of 50%–60% of total cells.

Figure 2. IPSC-NCSCs Express Low Levels of HLA Class I, HLA Class II, and Costimulatory Molecules

(A) Representative histograms of % of cells positive for HLA class I and class II and costimulatory molecules, including CD40, CD80, and CD86. Percentages are of total NIBSC8-NCSCs as untreated, after IFN-γ alone, TNF-α, or combined IFN-γ + TNF-α treatment (black line versus gray graph of isotype control). (B) Graphs of % of cells positive for HLA class I and class II and costimulatory molecules in NIBSC8 iPSCs, NIBSC8-NCSCs, NIBSC35-NCSCs, and NIBSC8-SMCs. Error bars represent ± SEM (n = 3 biological replicates per cell line and condition). Ordinary one-way ANOVA with Bonferroni post-test was performed. Asterisks denote statistical significance: $^*p \leq 0.05$, $^{**}p \leq 0.01$, and $^{***}p \leq 0.001$. Only relevant statistics are shown in the graphs.

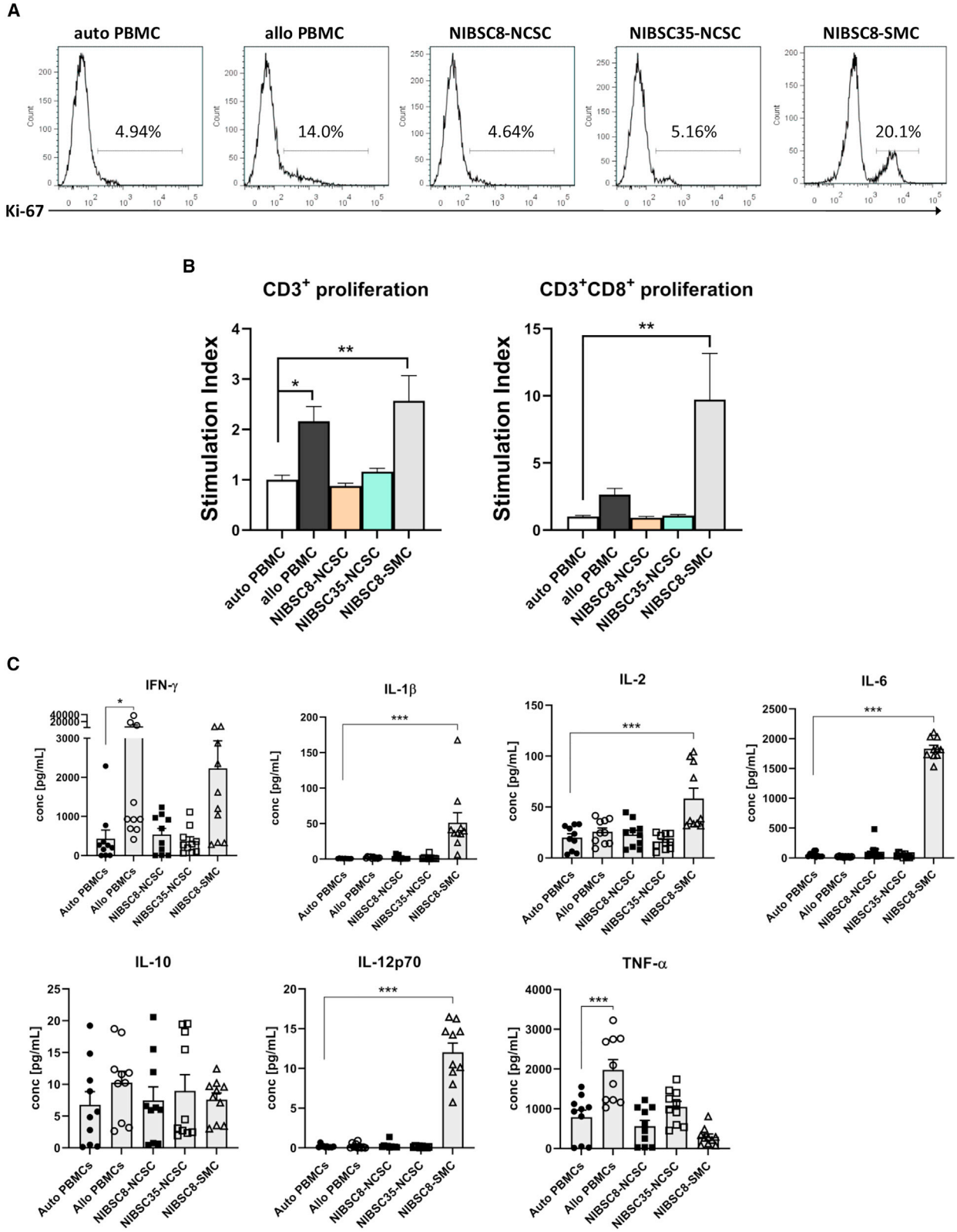

(legend on next page)

To characterize the immune profile of iPSC-NCSCs, we evaluated the expression of HLA class I and II as the main mediators of immunogenicity. We showed that basal expression of HLA class I and II is low, and iPSC-NCSCs also express low levels of co-stimulatory molecules. This molecular phenotype therefore suggests that iPSC-NCSCs exhibit low immunogenicity and antigen-presenting function in a non-inflammatory environment. To investigate further whether iPSC-NCSCs can activate T cells on a functional level, we used a one-way MLR to measure T cell proliferation. Correlating with their non-immunogenic molecular phenotype, iPSC-NCSCs from both iPSC lines failed to activate T cells above basal level, whereas an alternative cell type (SMCs) derived from the same iPSC line caused a significant elevation in T cell proliferation, further supporting the theory that the immunogenicity of iPSC derivatives depends on the differentiated cell type.

To further investigate the negligible immunogenicity of iPSCs-NCSCs, we assessed cytokine release in co-cultures with PBMCs. The significance of different cytokines in allograft tolerance/rejection is widely known. For instance, the presence of T cells secreting "type 1" cytokines, such as IFN-γ and TNF-α, tends toward a hostile environment for graft survival.[31] Moreover, IL-6 deficiency results in a decrease of peripheral memory T cells and prolonged allograft survival in a transplant model.[32] IL-12 within inflammatory tissue sites has been associated with provoking infiltrating memory $CD8^+$ T cells to proliferate and express effector function, including IFN-γ and TNF-α production, as well as perforin/granzyme B-mediated cytolysis.[33] Here we showed that iPSC-derived NCSCs did not induce IFN-γ and TNF-α production, characteristic for a "type 1" proinflammatory T cell response. Other proinflammatory cytokines, including IL-1β, IL-6, and IL-12p70, were induced by iPSC-SMCs, but not by iPSC-NCSCs. This suggests that iPSC-NCSCs not only fail to stimulate T cell proliferation, but more specifically, do not induce T cells to produce proinflammatory cytokines that are known to contribute to graft rejection. The immune response to iPSC-SMCs is not discussed in depth here, although it should be noted that the relatively modest levels of expression of co-stimulatory molecules by iPSC-SMCs are inconsistent with the highly immunogenic phenotype seen in functional assays. However, this may be partially explained by the expression of tumor-related antigens and/or *de novo* mutations in mitochondrial DNA, which has previously been suggested for this cell type.[10,34]

Data from multiplex immunoassays also revealed that iPSC-NCSCs did not induce IL-10 expression from PBMCs, which has been associated with low immunogenicity of iPSCs.[22] Although the inability to induce IL-10 production suggests that iPSC-NCSCs are not immunosuppressive, we further investigated whether iPSC-NCSCs exert immunosuppressive features when exposed to highly stimulated lymphocytes. Here, we showed that iPSC-NCSCs do not suppress proliferation of total $CD3^+$ T cells or $CD3^+CD8^+$ T cells, whereas MSCs differentiated from the same iPSC line elicited a significant reduction in T cell proliferation to similar levels as immunosuppressive BM-MSCs. This supports our finding of negligible immunogenicity of iPSC-NCSCs, which can indeed be attributed to their immune profile, rather than an immunosuppressive phenotype.

Although this first report on the immune profile of iPSC-derived NCSCs provides a robust body of evidence for their low immunogenicity, it should be noted that it cannot be excluded that this may be a result of the relative embryonic phenotype of iPSC-NCSCs. Moreover, it is expected that the therapeutic benefit of these cells is likely to be dependent on the *in vivo* differentiation capacity of iPSC-NCSCs. As has been suggested by two studies, ESC-derived NCSCs and iPSC-NCSCs further differentiated into peripheral neurons[16] and Schwann cells,[18] respectively, after transplantation. At the same time, this also highlights the importance of characterizing the immune profile of these progenitors, because in this instance, it is not the terminally differentiated cells but rather the NCSCs that represent the transplanted graft. The fact that further differentiation in the host is expected with this cell type reinforces that subsequent *in vivo* studies will be essential to validate our findings of low immunogenicity of iPSC-NCSCs. In addition, the lack of basal HLA class I molecule expression in iPSC-NCSCs may render them a target of natural killer (NK) cells, according to the "missing-self" hypothesis.[35] Although the lack of proinflammatory cytokine production may give some indication for a low responsiveness of NK cells toward iPSC-NCSCs (whole PBMCs served as responder cells), due to the low percentage of NK cells in PBMCs, this would need to be validated in an assay using isolated NK cells only as responder cells.

In conclusion, this study has demonstrated that iPSC-NCSCs are non-immunogenic *in vitro*. These results are encouraging for the potential future use of iPSC-NCSCs as a cellular therapy, perhaps in a strategy where they are subject to further "maturation" toward a more differentiated phenotype in the *in vivo* environment, because it suggests that these cells might be "immune-privileged" and not subject to allograft rejection by the recipient.

Figure 3. IPSC-NCSCs Fail to Stimulate Lymphocytes

(A) Representative histograms show levels of $CD3^+CD8^+$ T cell proliferation of responder cells after 5-day co-culture with autologous (auto), allogeneic (allo) PBMCs, NIBSC8-NCSCs, NIBSC35-NCSCs, or NIBSC8-SMCs as stimulator cells. (B) Graphs show stimulation index (SI) of total T cell ($CD3^+$) and $CD3^+CD8^+$ T cell proliferation in the responder cell population in response to different stimulator cells. SI is calculated as the number of $Ki67^+$ cells of each one-way MLR over the number of $Ki67^+$ cells in an autologous control. Numbers are expressed relative to the control group: autologous (auto) PBMCs. A response was considered positive when the SI was ≥ 2. Error bars represent ± SEM (n = 11 biological replicates from three separate experiments). Ordinary one-way ANOVA with Bonferroni post-test was performed. Asterisks denote statistical significance: $^*p \leq 0.05$, $^{**}p \leq 0.01$, $^{***}p \leq 0.001$. (C) Supernatants of 5-day co-cultures were assayed for IFN-γ, IL-1β, IL-2, IL-6, IL-10, IL12-p70, and TNF-α using multiplex immunoassays. Error bars represent ± SEM (n = 10 biological replicates from three separate experiments). Ordinary one-way ANOVA with Bonferroni post-test was performed. Asterisks denote statistical significance: $^*p \leq 0.05$, $^{**}p \leq 0.01$, and $^{***}p \leq 0.001$. Only statistically significant comparisons are shown in the graphs.

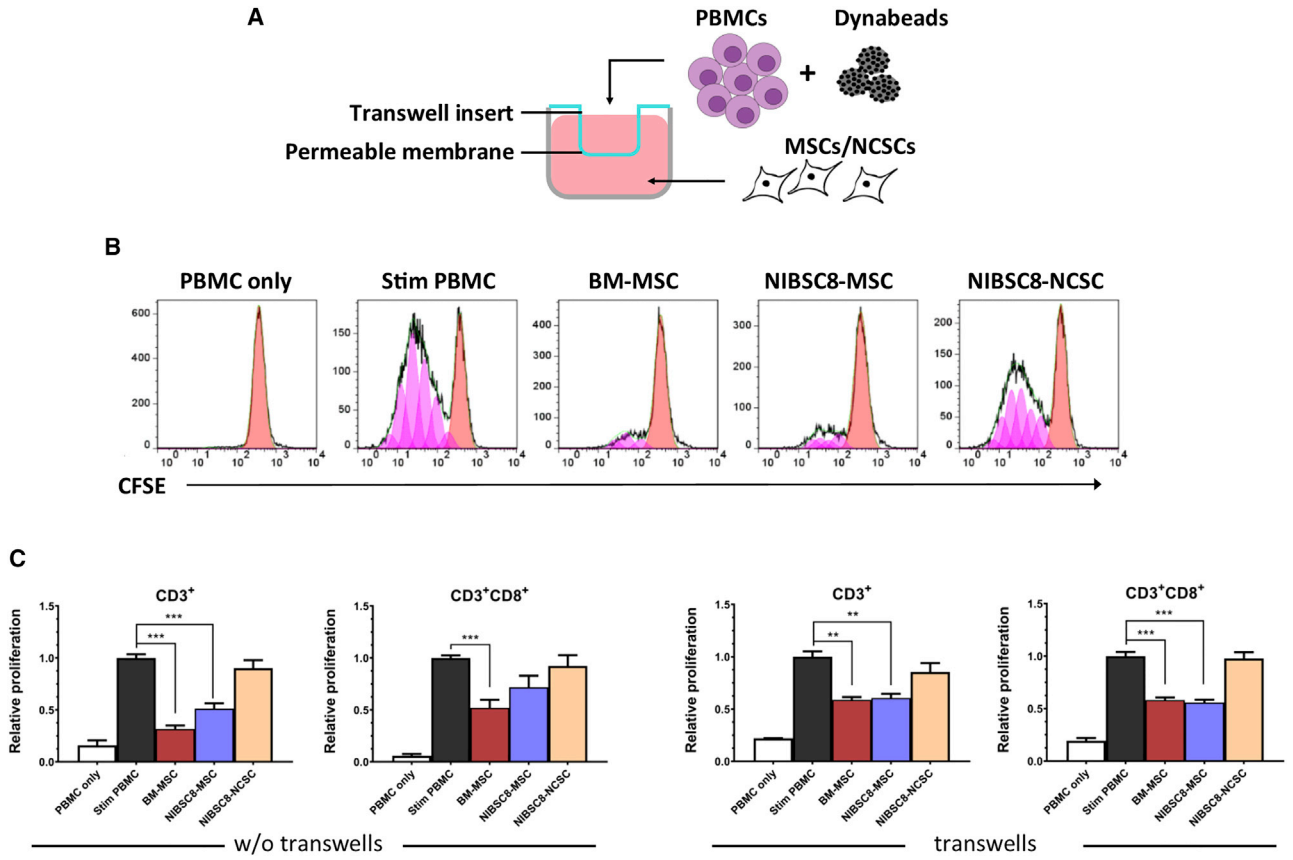

Figure 4. IPSC-NCSCs Are Not Immunosuppressive

(A) Schematic outline of transwell assay format. (B) Representative flow cytometry histograms show T cell proliferation, detected by quantifying levels of CFSE by flow cytometry. Anti-CD3/anti-CD28-stimulated PBMCs were co-cultured with BM-MSCs, NIBSC8-MSCs, and NIBSC8-NCSCs, and reduction of T cell proliferation was measured by quantifying $CFSE^{low}$ cells (shown in pink) in total $CD3^+$ T cells and $CD3^+CD8^+$ T cells. (C) Graphs show relative total $CD3^+$ T cell and $CD3^+CD8^+$ T cell proliferation in a transwell assay format (tw) and without transwell inserts (w/o tw). Bars represent proliferation in PBMCs only, in stimulated (stim) PBMCs only, and in stim PBMCs in response to co-culture with BM-MSCs, NIBSC8-MSCs, and NIBSC8-NCSCs relative to stim PBMCs. Error bars represent ± SEM (w/o tw: n = 9 biological replicates in three separate experiments; with tw: n = 3 biological replicates in a single experiment). Ordinary one-way ANOVA with Bonferroni post-test was performed. Asterisks denote statistical significance in comparison with stim PBMCs: *$p \leq 0.05$, **$p \leq 0.01$, and ***$p \leq 0.001$.

MATERIALS AND METHODS

Cell Culture

Human cell lines were handled in accordance with the Human Tissue Act (2004) with approval from The Human Materials Advisory Committee (HuMAC) at the National Institute for Biological Standard and Control. The NIBSC8 iPSC line was generously donated by the UK Stem Cell Bank (NIBSC8 was generated by mRNA-based reprogramming of human fibroblasts). NIBSC35 was generated from human PBMCs using the CytoTune−iPS 2.0 Sendai Reprogramming Kit (A16518; Thermo Fisher), according to the manufacturer's instructions with some modifications from a previously published protocol.[36] Characterization results are supplied as Supplemental Information (Figure S5). IPSCs were maintained in an undifferentiated pluripotent state in Essential 8 Flex (Life Technologies) media on Vitronectin (GIBCO)-coated plates. Media were changed every other day, and iPSCs were passaged every 4–5 days using Versene Solution (GIBCO). To test the potential to differentiate into all three germ layers, an embryoid body (EB) formation assay was performed with subsequent spontaneous differentiation for 14 days. AggreWell400 microwell plates (STEMCELL Technologies) were used to form EBs from single-cell suspension of pluripotent iPSCs at a concentration of 1.2×10^6 cells/well and according to the manufacturer's instructions (Figure S4). NCSCs were differentiated from iPSCs as described previously.[17] In brief, iPSCs were dissociated and plated as single-cell suspensions onto Vitronectin-coated six-well plates in Essential 6 Medium (Life Technologies) supplemented with 10 μM γ-27632 (Sigma-Aldrich) at a density of 10,000 cells/cm^2. Twenty-four hours after seeding, the medium was changed to NCSC media, consisting of Essential 6 Medium, N2 supplement (Thermo Fisher), 1 μM CHIR99021 (Sigma-Aldrich), 2 μM SB431542 (Sigma-Aldrich), 15 ng/mL recombinant Bone Morphogenetic Protein 4 (BMP4; R&D Systems), and 1 μM DMH-1 (R&D Systems). Differentiation to NCSCs was completed after 7 days. To achieve a higher yield of $HNK1^+p75^{high}$ cells for NIBSC35, NCSC differentiation was followed

by NCSC rosette isolation using STEMdiff Neural Rosette Selection Reagent (STEMCELL Technologies), according to the manufacturer's instructions. SMCs were differentiated from iPSCs as described previously,[37] and MSCs were generated from iPSCs as described in previously published protocols.[13] Peripheral nerve differentiation was performed as described previously for NIBSC8[13] and with slight modifications (substitution with NCSC media as described above; reduced incubation time) for NIBSC35. For DC generation, $CD14^+$ monocytes were isolated from PBMCs by negative selection using the EasySep Human Monocyte Enrichment Kit (STEMCELL Technologies) according to the manufacturer's instructions, followed by 7-day culture in RPMI 1640 supplemented with 10% fetal calf serum (FCS), 2 mM glutamine, 2 mM L-glutamine, 50 U/mL penicillin/streptomycin, 20 ng/mL granulocyte-macrophage colony-stimulating factor (GM-CSF), and 20 ng/mL IL-4. BM-MSCs were derived from bone marrow aspirates (AllCells, Alameda, CA, USA) in-house as previously described.[38] Vessel-derived SMCs were kindly provided by George Tellides (Yale University, School of Medicine) and were maintained in Medium 199 (Sigma-Aldrich), 20% heat-inactivated FCS, 2 mM L-glutamine, 100 U/mL penicillin, and 100 μg/mL streptomycin. To induce immune-related antigen expression on iPSCs and derivatives, we treated cells with 25 ng/mL IFN-γ (R&D Systems) and/or 10 ng/mL TNF-α (R&D Systems) in indicated medium for 48 h and then analyzed for immune-related antigen expression.

Flow Cytometry

IPSCs, iPSC derivatives, and somatic cells were dissociated using ACCUTASE (for adherent cell cultures). Cells were incubated with the indicated conjugated antibody diluted to the appropriate concentration (Table S2) and incubated on ice for 30 min in the dark. Subsequently, cells were fixed with 4% paraformaldehyde (PFA) in PBS and either subjected to intracellular staining first using BD Cytofix/Cytoperm (catalog no. 554714; BD Biosciences) or immediately subjected to flow cytometric analysis using BD FACS Canto II (BD Biosciences). Data was analyzed using FlowJo 7.6.5.

qPCR Analysis

Total RNA was isolated from cell lysates using the RNeasy Mini Kit (QIAGEN) according to the manufacturer's instructions. First-Strand cDNA synthesis from RNA was performed using the M-MLV Reverse Transcriptase system (Promega), and the cDNA product was subject to qPCR using 2× qPCRBIO SyGreen Blue Mix Lo-ROX (PCRBiosystem) and pre-designed primers (purchased from Integrated DNA Technologies [IDT], details in Table S3). The qPCRs were performed on a Rotor-Gene Q thermocycler, and data were analyzed using the Rotor-Gene Q System (QIAGEN), software version: 2.1.0. Target gene expression was normalized to *GAPDH* expression and is referred to as normalized expression.

One-Way MLR

To assess and compare the immunogenic potential of iPSC-derived cells, we used a one-way MLR assay. PBMCs were used as responder cells, and autologous PBMCs, allogeneic PBMCs, iPSC-NCSCs, or iPSC-SMCs served as stimulators, respectively. Co-cultures were maintained in complete RPMI media (RPMI 1640 supplemented with 10% FCS, 2 mM L-glutamine, 50 U/mL penicillin/streptomycin). A total of 3×10^5 responder cells were co-cultured with 1.5×10^5 UV irradiated stimulator cells and maintained in 200 μL of complete RPMI media in 96-well plates at 37°C in 5% CO_2 for 5 days. To specifically assess T cell proliferation of responders, we labeled cells with fixable viability dye (FVD), T cell markers, and anti-Ki-67 (Table S2). The expression of the human Ki-67 protein is strictly associated with cell proliferation,[39] and thus $Ki\text{-}67^+$ cells denote proliferating cells. Levels of proliferation were numerically expressed as SI, calculated as the number of $Ki67^+$ cells of each one-way MLR over the number of $Ki67^+$ cells in an autologous control. A response was considered positive when the SI was ≥ 2.[23,24]

Mesoscale Multiplex Cytokine Immunoassay

Cytokine concentrations from 5-day co-cultures were quantified using V-PLEX human cytokine 10-plex kit (Mesoscale) detecting IFN-γ, IL-1β, IL-2, IL-6, IL-10, IL-12p70, and TNF-α analytes. Supernatants were processed according to the manufacturer's protocol, and the electrochemiluminescent signal was detected by MESO QuickPlex SQ 120. Analysis of results was carried out using the MSD DISCOVERY WORKBENCH analysis software, including calculations to establish calibration curves and determining concentrations.

Immunosuppression Assay

To investigate whether iPSC-derived cells have an immunosuppressive effect *in vitro*, we used an immunosuppression assay. Putative immunosuppressive cells (BM-MSCs, iPSC-MSCs, and iPSC-NCSCs) were plated at a density of 5×10^4 cells/well onto a 24-well plate and maintained in appropriate media overnight. The following day, responder cells (PBMCs) were stained with CellTrace CSFE (Invitrogen) to measure proliferation and added to putative immunosuppressive cells at a concentration of 1×10^6 cells/well. PBMCs were stimulated with anti-CD3/anti-CD28 Dynabeads (Invitrogen) at a dilution of 1:1,000. In addition, an immunosuppression assay using a tw with a permeable membrane was also performed. This assay system facilitates molecule exchange but not cell-to-cell contact, enabling measurement of immunosuppression mediated via soluble factors only. Putative immunosuppressive cells were maintained in the lower compartment of Corning Transwell polyester membrane cell culture inserts (Sigma-Aldrich) in 24-well plates, with PBMCs in the upper compartment (within the insert). The co-culture was maintained in complete RPMI at 37°C in 5% CO_2 for 4 days before analysis by flow cytometry. T cell proliferation was analyzed as per MLR above (see Table S2). Levels of T cell proliferation in co-cultures were expressed relative to the PBMC positive control (stimulated with Dynabeads).

Immunocytochemistry

Immunocytochemistry (ICC) was performed on fixed (4% PFA) cells. The primary antibody was diluted to the appropriate concentration (see Table S4) in PBST buffer (0.1% Triton X-100 [Sigma-Aldrich] in PBS) and incubated overnight at 4°C in the dark. Cells were washed

in PBST and then incubated with the respective secondary antibody (Table S4) in PBST at room temperature for 1 h in the dark. Cells were washed in PBST to remove excess antibody and then stained with Hoechst 33342 nuclear stain (Invitrogen) at a concentration of 5 μg/mL in PBS for 1 min at room temperature. Fixed and stained cells were imaged with a White Light Laser Confocal Microscope Leica SP8 X confocal laser scanning microscope (CLSM) (Leica Microsystems). The imaging software Fiji: An Open-Source Platform for Biological-Image Analysis (Version 1.51) was used for image analysis.

Statistical Analysis

Values were expressed as mean ± SEM (standard error of the mean). The significance of differences among multiple groups was determined with a one-way analysis of variance (ANOVA) followed by a Bonferroni post-test (GraphPad Prism version 8.2.1). Differences were considered significant where $p < 0.05$. Significance levels are defined as follows: $^{*}p \leq 0.05$, $^{**}p \leq 0.01$, and $^{***}p \leq 0.001$.

SUPPLEMENTAL INFORMATION

Supplemental Information can be found online at https://doi.org/10.1016/j.omtm.2019.12.015.

AUTHOR CONTRIBUTIONS

Conceptualization, V.J.M., M.L.M., and C.J.B.; Methodology, V.J.M., M.L.M., and C.J.B.; Formal Analysis, V.J.M.; Investigation, V.J.M., M.L.M., and R.J.F.; Writing – Original Draft, V.J.M.; Writing – Review & Editing, V.J.M., M.L.M., C.J.B., and H.S.; Visualization, V.J.M.; Supervision, M.L.M., C.J.B., and H.S.; Project Administration V.J.M., M.L.M., and C.J.B.; Funding Acquisition, C.J.B.

CONFLICTS OF INTEREST

The authors declare no competing interests.

ACKNOWLEDGMENTS

This work was funded in part by UK Department of Health's Policy Research Programme grant number 044/0069. The report is based on independent research commissioned and funded by the NIHR Policy Research Programme, Regulatory Science Research Unit (RSRU). The views expressed in the publication are those of the authors and not necessarily those of the NHS, the NIHR, the Department of Health, "arms" length bodies, or other government departments.

REFERENCES

1. Aoi, T., and Stacey, G. (2015). Impact of National and International Stem Cell Banking Initiatives on progress in the field of cell therapy: IABS-JST Joint Workshop: Summary for Session 5. Biologicals *43*, 399–401.

2. Zimmermann, A., Preynat-Seauve, O., Tiercy, J.M., Krause, K.H., and Villard, J. (2012). Haplotype-based banking of human pluripotent stem cells for transplantation: potential and limitations. Stem Cells Dev. *21*, 2364–2373.

3. Japan Agency for Medical Research and Development (2018). The world's first allogeneic iPS-derived retina cell transplant. https://www.amed.go.jp/en/seika/fy2018-05.html.

4. UMIN-CTR Clinical Trial (2018). Kyoto trial to evaluate the safety and efficacy of iPSC-derived dopaminergic progenitors in the treatment of Parkinson's disease. https://hpscreg.eu/browse/trial/54.

5. Ozaki, M., Iwanami, A., Nagoshi, N., Kohyama, J., Itakura, G., Iwai, H., Nishimura, S., Nishiyama, Y., Kawabata, S., Sugai, K., et al. (2017). Evaluation of the immunogenicity of human iPS cell-derived neural stem/progenitor cells in vitro. Stem Cell Res. (Amst.) *19*, 128–138.

6. Chhabra, A., Chen, I.-P., and Batra, D. (2017). Human Dendritic Cell-Derived Induced Pluripotent Stem Cell Lines Are Not Immunogenic. J. Immunol. *198*, 1875–1886.

7. Kimura, T., Yamashita, A., Ozono, K., and Tsumaki, N. (2016). Limited Immunogenicity of Human Induced Pluripotent Stem Cell-Derived Cartilages. Tissue Eng. Part A *22*, 1367–1375.

8. Schnabel, L.V., Abratte, C.M., Schimenti, J.C., Felippe, M.J.B., Cassano, J.M., Southard, T.L., Cross, J.A., and Fortier, L.A. (2014). Induced pluripotent stem cells have similar immunogenic and more potent immunomodulatory properties compared with bone marrow-derived stromal cells in vitro. Regen. Med. *9*, 621–635.

9. Kawamura, T., Miyagawa, S., Fukushima, S., Maeda, A., Kashiyama, N., Kawamura, A., Miki, K., Okita, K., Yoshida, Y., Shiina, T., et al. (2016). Cardiomyocytes Derived from MHC-Homozygous Induced Pluripotent Stem Cells Exhibit Reduced Allogeneic Immunogenicity in MHC-Matched Non-human Primates. Stem Cell Reports *6*, 312–320.

10. Zhao, T., Zhang, Z.N., Westenskow, P.D., Todorova, D., Hu, Z., Lin, T., Rong, Z., Kim, J., He, J., Wang, M., et al. (2015). Humanized Mice Reveal Differential Immunogenicity of Cells Derived from Autologous Induced Pluripotent Stem Cells. Cell Stem Cell *17*, 353–359.

11. Araki, R., Uda, M., Hoki, Y., Sunayama, M., Nakamura, M., Ando, S., Sugiura, M., Ideno, H., Shimada, A., Nifuji, A., and Abe, M. (2013). Negligible immunogenicity of terminally differentiated cells derived from induced pluripotent or embryonic stem cells. Nature *494*, 100–104.

12. Chen, H.-F., Yu, C.-Y., Chen, M.-J., Chou, S.-H., Chiang, M.-S., Chou, W.-H., Ko, B.-S., Huang, H.-P., Kuo, H.-C., and Ho, H.-N. (2015). Characteristic expression of major histocompatibility complex and immune privilege genes in human pluripotent stem cells and their derivatives. Cell Transplant. *24*, 845–864.

13. Menendez, L., Kulik, M.J., Page, A.T., Park, S.S., Lauderdale, J.D., Cunningham, M.L., and Dalton, S. (2013). Directed differentiation of human pluripotent cells to neural crest stem cells. Nat. Protoc. *8*, 203–212.

14. Zhu, Q., Lu, Q., Gao, R., and Cao, T. (2016). Prospect of human pluripotent stem cell-derived neural crest stem cells in clinical application. Stem Cells Int. *2016*, 7695836.

15. Achilleos, A., and Trainor, P.A. (2012). Neural crest stem cells: discovery, properties and potential for therapy. Cell Res. *22*, 288–304.

16. Curchoe, C.L., Maurer, J., McKeown, S.J., Cattarossi, G., Cimadamore, F., Nilbratt, M., Snyder, E.Y., Bronner-Fraser, M., and Terskikh, A.V. (2010). Early acquisition of neural crest competence during hESCs neuralization. PLoS ONE *5*, e13890.

17. Hackland, J.O.S., Frith, T.J.R., Thompson, O., Marin Navarro, A., Garcia-Castro, M.I., Unger, C., and Andrews, P.W. (2017). Top-Down Inhibition of BMP Signaling Enables Robust Induction of hPSCs Into Neural Crest in Fully Defined, Xeno-free Conditions. Stem Cell Reports *9*, 1043–1052.

18. Wang, A., Tang, Z., Park, I.-H., Zhu, Y., Patel, S., Daley, G.Q., and Li, S. (2011). Induced pluripotent stem cells for neural tissue engineering. Biomaterials *32*, 5023–5032.

19. Xu, W., Wang, Y., Liu, E., Sun, Y., Luo, Z., Xu, Z., Liu, W., Zhong, L., Lv, Y., Wang, A., et al. (2013). Human iPSC-derived neural crest stem cells promote tendon repair in a rat patellar tendon window defect model. Tissue Eng. Part A *19*, 2439–2451.

20. Liu, Q., Spusta, S.C., Mi, R., Lassiter, R.N., Stark, M.R., Höke, A., Rao, M.S., and Zeng, X. (2012). Human neural crest stem cells derived from human ESCs and induced pluripotent stem cells: induction, maintenance, and differentiation into functional schwann cells. Stem Cells Transl. Med. *1*, 266–278.

21. Deuse, T., Hu, X., Gravina, A., Wang, D., Tediashvili, G., De, C., Thayer, W.O., Wahl, A., Garcia, J.V., Reichenspurner, H., et al. (2019). Hypoimmunogenic derivatives of induced pluripotent stem cells evade immune rejection in fully immunocompetent allogeneic recipients. Nat. Biotechnol. *37*, 252–258.

22. Lu, Q., Yu, M., Shen, C., Chen, X., Feng, T., Yao, Y., Li, J., Li, H., and Tu, W. (2014). Negligible immunogenicity of induced pluripotent stem cells derived from human skin fibroblasts. PLoS ONE *9*, e114949.

23. Du Pasquier, L., and Weiss, N. (1973). The thymus during the ontogeny of the toad Xenopus laevis: growth, membrane-bound immunoglobulins and mixed lymphocyte reaction. Eur. J. Immunol. *3*, 773–777.

24. Ringdén, O., Möller, E., Lundgren, G., and Groth, C.G. (1976). Role of MLC compatibility in intrafamilial kidney transplantation. Transplantation *22*, 9–17.

25. Di Nicola, M., Carlo-Stella, C., Magni, M., Milanesi, M., Longoni, P.D., Matteucci, P., Grisanti, S., and Gianni, A.M. (2002). Human bone marrow stromal cells suppress T-lymphocyte proliferation induced by cellular or nonspecific mitogenic stimuli. Blood *99*, 3838–3843.

26. Bartholomew, A., Sturgeon, C., Siatskas, M., Ferrer, K., McIntosh, K., Patil, S., Hardy, W., Devine, S., Ucker, D., Deans, R., et al. (2002). Mesenchymal stem cells suppress lymphocyte proliferation in vitro and prolong skin graft survival in vivo. Exp. Hematol. *30*, 42–48.

27. Nauta, A.J., Kruisselbrink, A.B., Lurvink, E., Willemze, R., and Fibbe, W.E. (2006). Mesenchymal stem cells inhibit generation and function of both CD34+-derived and monocyte-derived dendritic cells. J. Immunol. *177*, 2080–2087.

28. Li, C.-L., Leng, Y., Zhao, B., Gao, C., Du, F.-F., Jin, N., Lian, Q.-Z., Xu, S.-Y., Yan, G.-L., Xia, J.-J., et al. (2017). Human iPSC-MSC-Derived Xenografts Modulate Immune Responses by Inhibiting the Cleavage of Caspases. Stem Cells *35*, 1719–1732.

29. Sun, Y.Q., Zhang, Y., Li, X., Deng, M.X., Gao, W.X., Yao, Y., Chiu, S.M., Liang, X., Gao, F., Chan, C.W., et al. (2015). Insensitivity of Human iPS Cells-Derived Mesenchymal Stem Cells to Interferon-γ-induced HLA Expression Potentiates Repair Efficiency of Hind Limb Ischemia in Immune Humanized NOD Scid Gamma Mice. Stem Cells *33*, 3452–3467.

30. Betters, E., Liu, Y., Kjaeldgaard, A., Sundström, E., and García-Castro, M.I. (2010). Analysis of early human neural crest development. Dev. Biol. *344*, 578–592.

31. Ferrara, J.L. (1998). The cytokine modulation of acute graft-versus-host disease. Bone Marrow Transplant. *21* (*Suppl 3*), S13–S15.

32. Chen, J., Liu, C., Liu, B., Kong, D., Wen, L., and Gong, W. (2018). Donor IL-6 deficiency evidently reduces memory T cell responses in sensitized transplant recipients. Transpl. Immunol. *51*, 66–72.

33. Su, C.A. (2016). Transplant Immunology (John Wiley & Sons).

34. Deuse, T., Hu, X., Agbor-Enoh, S., Koch, M., Spitzer, M.H., Gravina, A., Alawi, M., Marishta, A., Peters, B., Kosaloglu-Yalcin, Z., et al. (2019). De novo mutations in mitochondrial DNA of iPSCs produce immunogenic neoepitopes in mice and humans. Nat. Biotechnol. *37*, 1137–1144.

35. Ljunggren, H.-G., and Kärre, K. (1990). In search of the 'missing self': MHC molecules and NK cell recognition. Immunol. Today *11*, 237–244.

36. Seki, T., Yuasa, S., and Fukuda, K. (2012). Generation of induced pluripotent stem cells from a small amount of human peripheral blood using a combination of activated T cells and Sendai virus. Nat. Protoc. *7*, 718–728.

37. Yang, L., Geng, Z., Nickel, T., Johnson, C., Gao, L., Dutton, J., Hou, C., and Zhang, J. (2016). Differentiation of human induced-pluripotent stem cells into smooth-muscle cells: two novel protocols. PLoS ONE *11*, e0147155.

38. Sekiya, I., Larson, B.L., Smith, J.R., Pochampally, R., Cui, J.G., and Prockop, D.J. (2002). Expansion of human adult stem cells from bone marrow stroma: conditions that maximize the yields of early progenitors and evaluate their quality. Stem Cells *20*, 530–541.

39. Scholzen, T., and Gerdes, J. (2000). The Ki-67 protein: from the known and the unknown. J. Cell. Physiol. *182*, 311–322.

OMTM, Volume *16*

Supplemental Information

Human iPSC-Derived Neural Crest Stem Cells Exhibit Low Immunogenicity

Vera J. Mehler, Chris J. Burns, Hans Stauss, Robert J. Francis, and Melanie L. Moore

Supplemental data

MSC differentiation

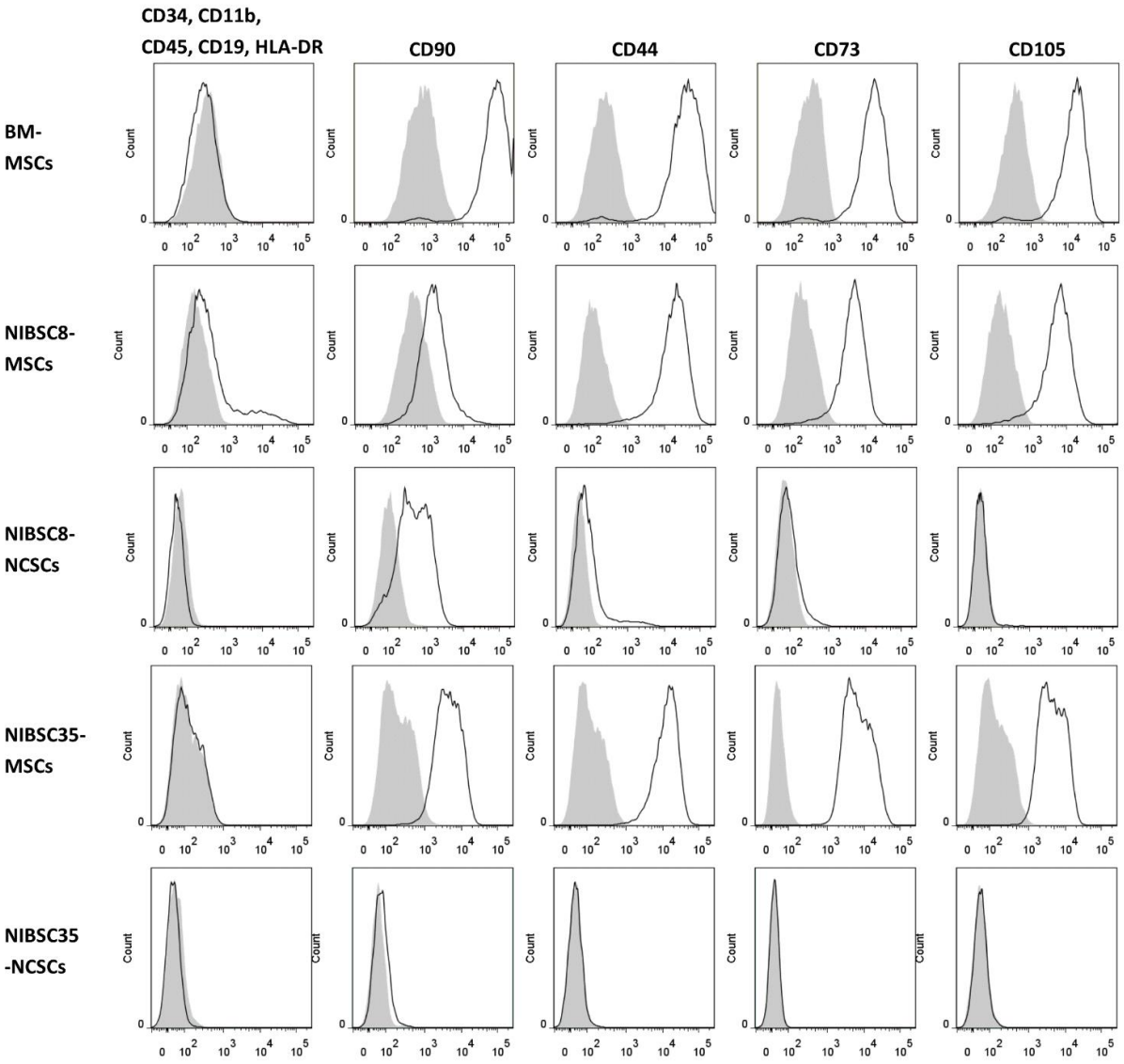

Figure S1. Characterisation of MSCs differentiated from iPSC-NCSCs. Representative histograms of % of cells positive for MSC markers, including CD90, CD44, CD73 and CD105 and MSC negative markers, including CD34, CD11b, CD45, CD19 and HLA-DR (black line vs grey shaded isotype control).

Peripheral nerve differentiation

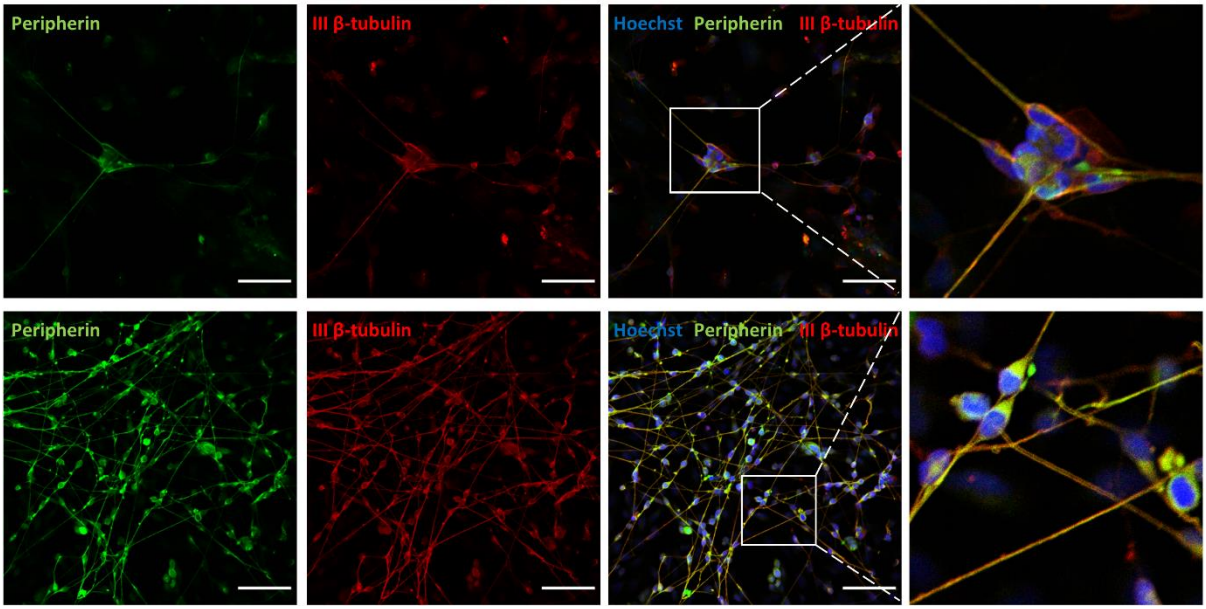

Figure S2. Characterisation of peripheral neurons generated from iPSC-NCSCs. Representative immunofluorescence staining of NIBSC8-NCSC-derived peripheral neurons (top row) and NIBSC35-NCSC-derived peripheral neurons (bottom row) with peripherin (green) and III β-tubulin (red). Hoechst staining was used to label the nuclei of the cells (blue). Scale bar = 100µm.

Dendritic cell differentiation

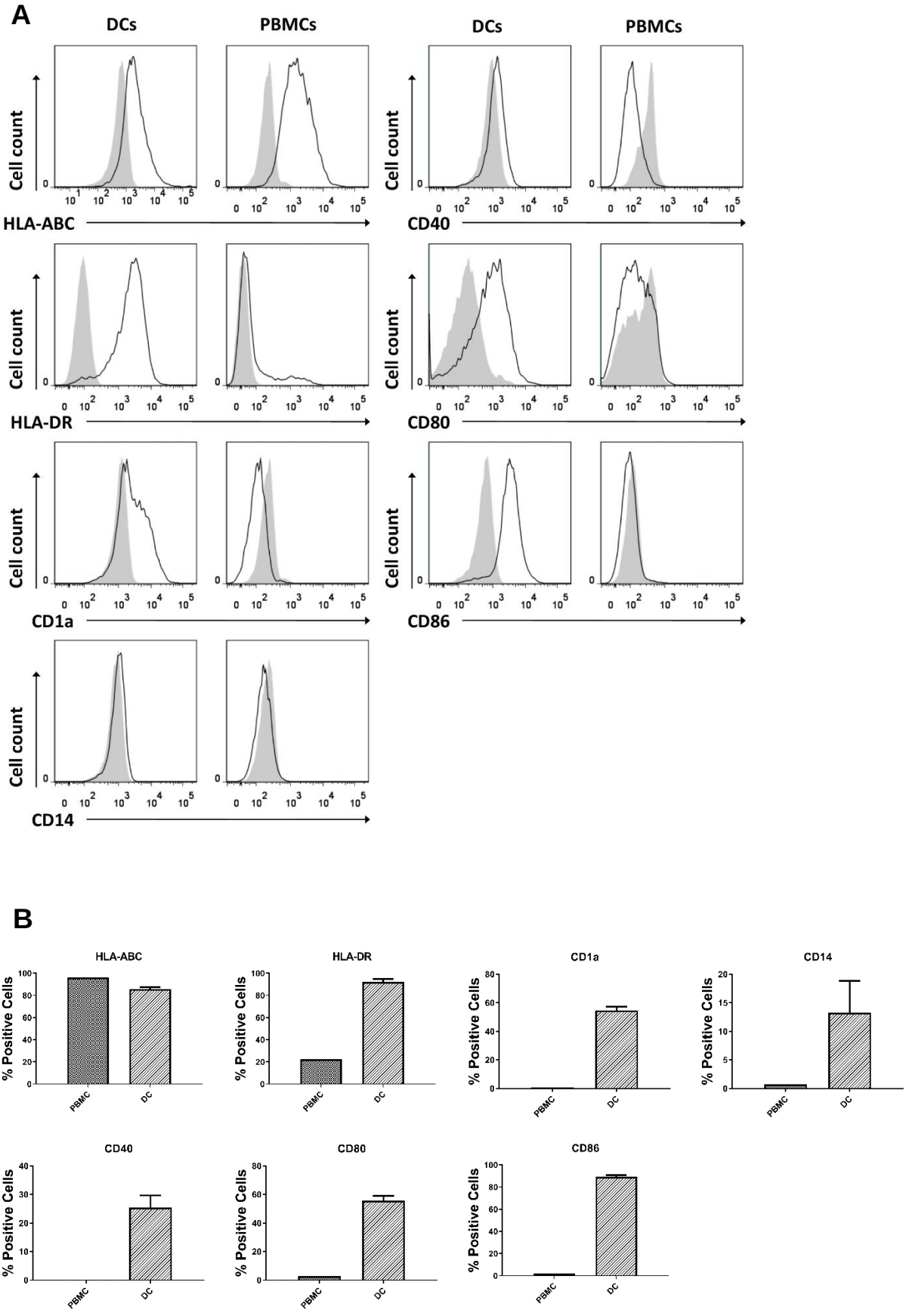

Figure S3. Dendritic cell generation from monocytes. (A) Representative histograms of % of cells positive for DC markers, including HLA-ABC, HLA-DR, CD1a, CD14, CD40, CD80 and CD86. Percentages are of total PBMCs and monocyte-derived DCs (black line vs grey shaded isotype control). (B) Graphs of % cells positive for DC markers in PBMCs and DCs. Error bars represent ±SEM (n = 3 technical replicates for DCs and n=1 technical replicate for PBMCs).

Smooth muscle cell differentiation

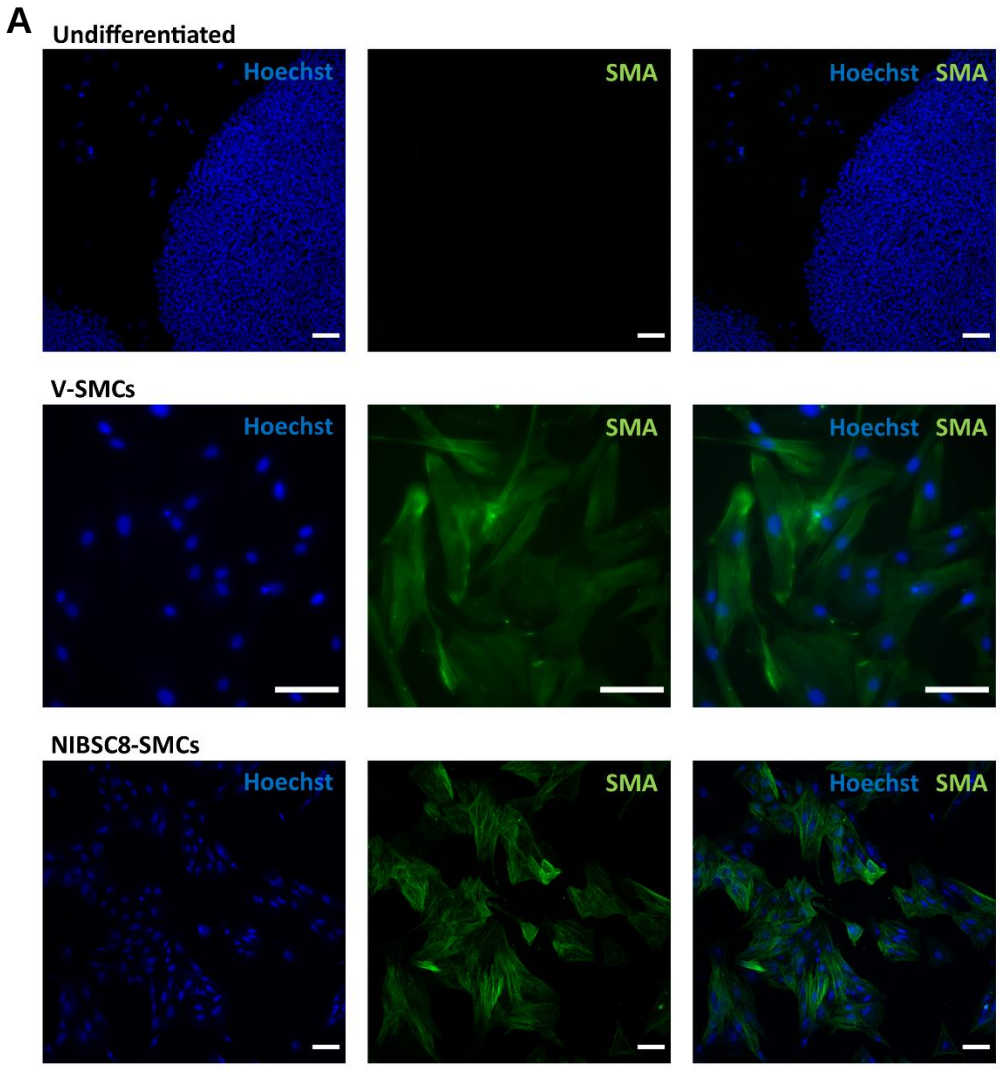

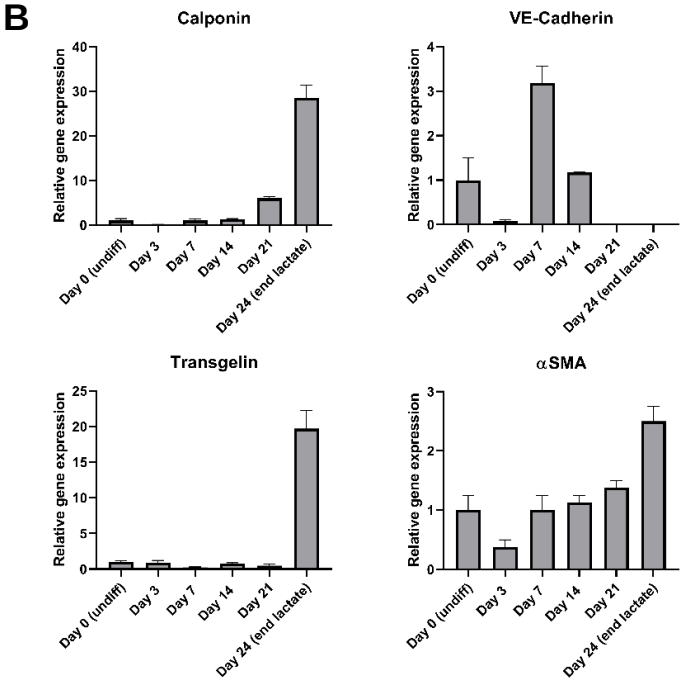

Figure S4. Characterisation of smooth muscle cells (SMCs) generated from iPSCs. (A) Representative immunofluorescence staining with smooth muscle actin (SMA, green) and Hoechst staining (blue) for undifferentiated iPSCs (NIBSC8), vessel-derived SMCs (v-SMCs) and NIBSC8-SMCs. Scale bar = 100µm. (B) cDNA was prepared from iPSCs at day 0 (undiff) and iPSC-SMCs at day 4 day 3, day 7, day 14, day 21 and day 24 (end of lactate=end of enrichment phase) of SMC differentiation and qPCR was performed for key SMC markers, including α*SMA*, *CALPONIN, TRANSGELIN* and for the endothelial marker *VE-CADHERIN.* Error bars represent ±SEM (n = 2 biological replicates). Results were normalised to *GAPDH* expressed as fold change gene expression relative to the undifferentiated control.

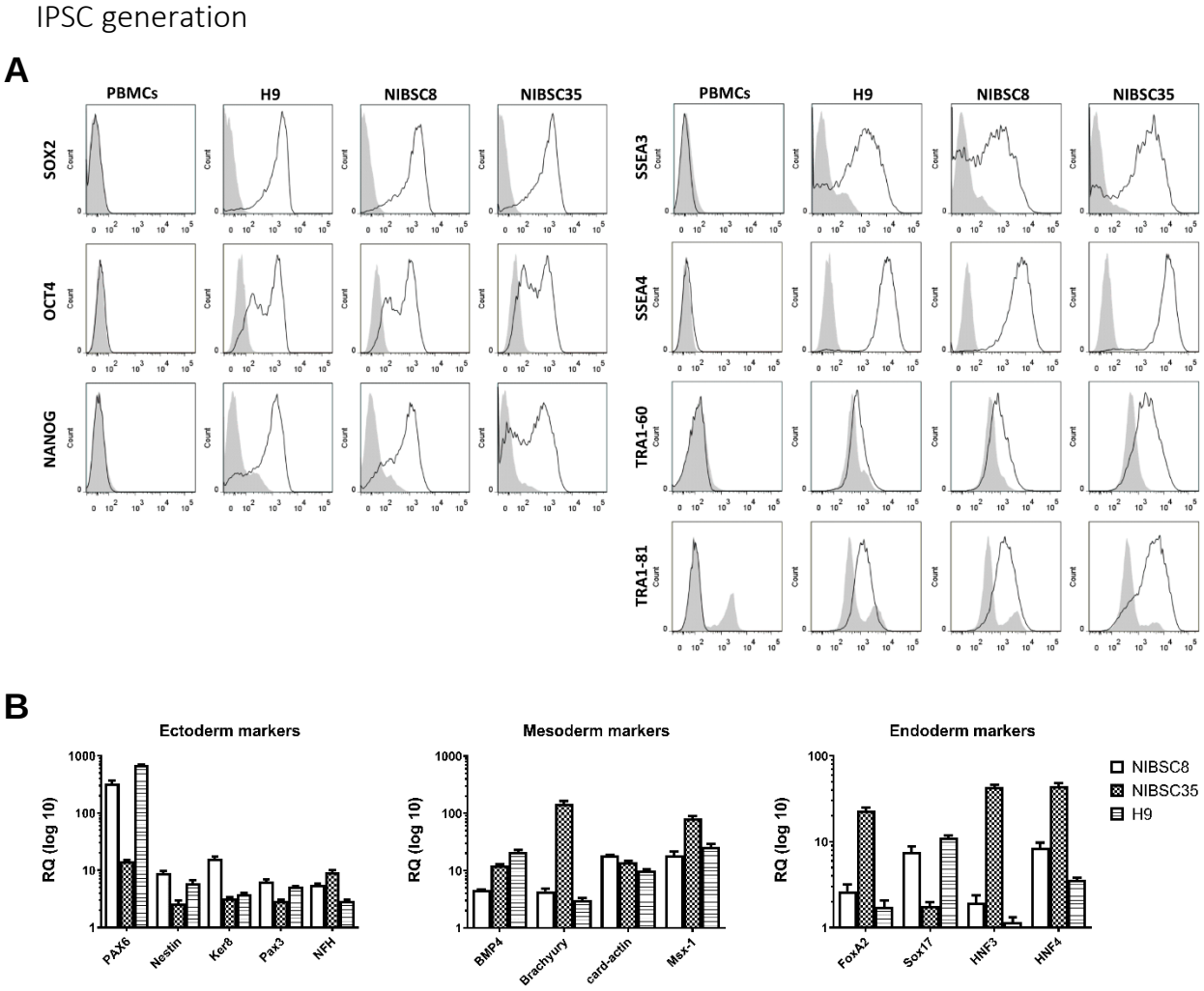

Figure S5. NIBSC8 and NIBSC35 iPSC characterisation. (A) Representative histograms of % of cells positive for pluripotency markers, including SOX2, OCT4, NANOG, SSEA3, SSEA4, TRA1-60 and TRA1-81. Percentages are of total PBMCs, H9 ES cells, NIBSC8 iPSCs and NIBSC35 iPSCs (black line vs grey shaded isotype control). (B) qPCR data from EBs, subject to 14 days of spontaneous differentiation, for expression of germ layer specific genes. The fold change in expression relative to the pluripotent control is shown (relative quantification, RQ). Error bars represent ±SEM (n = 3 biological replicates). Results were normalised to *GAPDH* expressed as fold change gene expression relative to the undifferentiated control.

Supplemental tables

Name	HLA-A	HLA-B	HLA- DRB1
IPSC lines:			
NIBSC8	*03 *23	*15 *44	*07 *13
NIBSC35	*02 *24	*08	*04 *15
PBMCs:			
Donor i	*26	*38 *35	*04 *04
Donor ii	*32 *29	*44 *27	*01 *08

Table S1: HLA types of stimulator and responder cell lines. The number after the asterisk represents an HLA allele (a blank number means that the line is homozygous for that allele). Antigen mismatch for NIBSC8 vs donor i is 6/6, mismatch for NIBSC8 vs donor ii is 5/6, mismatch for NIBSC35 vs donor i is 5/6 and mismatch for NIBSC35 vs donor ii is 6/6.

Specificity	Fluorochromes	Isotype	Clone	Staining dilution	Manufacturer, catalogue number
Surface markers:					
CD271/p75	PE	mouse IgG1	C40-1457	1:20	BD, 557196
HNK-1	APC	mouse IgG2a	NK-1	1:10	BD, 560845
CD3	Pacific Blue™	mouse IgG1	UCHT1	1:50	BD, 558117
CD4	APC-Cy™7	mouse IgG1	RPA-T4	1:50	BD, 557871
CD8	PerCP-Cy™5.5	mouse IgG1	RPA-T8	1:50	BD, 560662
HLA-ABC	PE	mouse IgG1	G46-2.6	1:25	BD, 560964
HLA-DR	APC	mouse IgG2a	L243	1:50	BioLegend, 307610
HLA-DR, DP, DQ	Alexa Fluor® 647	mouse IgG2a	Tu39	1:50	BD, 563591
CD40	V450	mouse IgG1	5C3	1:50	BD, 561219
CD80	PE-Cy™7	mouse IgG1	L307.4	1:50	BD, 561135
CD86	PerCP-Cy™5.5	mouse IgG1	2331	1:50	BD, 561129
CD1a	PE	mouse IgG1	HI149	1:10	BD, 555807
CD14	FITC	mouse IgG2a	M5E2	1:10	BD, 555397
SSEA3	Alexa Fluor® 647	rat IgM	MC-631	1:33	BD, 561145
SSEA4	PerCP-Cy™5.5	mouse IgG3	MC813-70	1:20	BD, 561565
TRA1-60	PE	mouse IgM	TRA-1-60	1:12.5	BD, 560884
TRA1-81	FITC	mouse IgM	TRA-1-81	1:5	BD, 560194
Human MSC Analysis Kit:					BD, 562245
CD90	FITC	mouse IgG1	5E10	1:20	n/a
CD105	PerCP-Cy™5.5	mouse IgG1	266	1:20	n/a
CD73	APC	mouse IgG1	AD2	1:20	n/a
CD44	PE	mouse IgG2b	G44-26	1:20	n/a
CD34	PE	mouse IgG1	581	1:20	n/a
CD11b	PE	mouse IgG1	ICRF44	1:20	n/a

CD19	PE	mouse IgG1	HIB19	1:20	n/a
CD45	PE	mouse IgG1	HI30	1:20	n/a
HLA-DR	PE	mouse IgG2a	G46-6	1:20	n/a
Intracellular markers:					
Ki-67	PE-Cy™7	mouse IgG1	B56	1:20	BD, 561283
SOX2	V450	mouse IgG1	O30-678	1:20	BD, 561610
OCT4	PerCP-Cy™5.5	mouse IgG1	40/Oct-3	1:25	BD, 560794
NANOG	Alexa Fluor® 647	mouse IgG1	N31-355	1:20	BD, 561300

Table S2: Antibodies used for flow cytometry. Summary of all antibodies used throughout this study for flow cytometry analysis.

No.	Primer	Primer Sequence	Annealing Temperature	PCR Product size
Pluripotency markers:				
3.	Oct4-F	GAC AGG GGG AGG GGA GGA GCT AGG	57 (°C)	143 bp
4.	Oct4-R	CTT CCC TCC AAC CAG TTG CCC CAA AC		
5.	Sox2-F	GGG AAA TGG GAG GGG TGC AAA AGA GG	57 (°C)	151 bp
6.	Sox2-R	TTG CGT GAG TGT GGA TGG GAT TGG TG		
7.	Nanog-F	TGC CTC ACA CGG AGA CTG TC	58 (°C)	65 bp
8.	Nanog-R	AGG GCT GTC CTG AAT AAG CA		
Housekeeping gene:				
13.	GAPDH-F	ACG AAT TTG GCT ACA GCA ACA GGG	56 (°C)	188 bp
14.	GAPDH-R	TCT ACA TGG CAA CTG TGA GGA GG		
Germ layer-specific markers:				
13.	PAX3-F	CGT CTC CAA GAT CCT GTG C	56 (°C)	91 bp
14.	PAX3-R	AGG CGT TGT CAC CTG CTT		
15.	PAX6-F	CCA GAA AGG ATG CCT CAT AAA GG	58 (°C)	50 bp
16.	PAX6-R	TCT GCG CGC CCC TAG TTA		
17.	KER8-F	TGA GGT CAA GGC ACA GTA CG	60 (°C)	161 bp
18.	KER8-R	TGA TGT TCC GGT TCA TCT CA		
19.	NFH-F	TGA ACA CAG ACG CTA TGC GCT CAG	58 (°C)	400 bp
20.	NFH-R	CAC CTT TAT GTG AGT GGA CAC AGA G		
21.	NESTIN-F	TGC GGG CTA CTG AAA AGT TC	58 (°C)	63 bp
22.	NESTIN-R	TGT AGG CCC TGT TTC TCC TG		
23.	BRACHYURY-F	TGC TTC CCT GAG ACC CAG TT	58 (°C)	121 bp
24.	BRACHYURY-R	GAT CAC TTC TTT CCT TTG CAT C		
25.	BMP4-F	CTG CAA CCG TTC AGA GGT C	58 (°C)	91 bp
26.	BMP4-R	TGC TCG GGA TGG CAC TAC		
27	Card-actin F	TCT ATG AGG GCT ACG CTT TG	50 (°C)	630 bp
28.	Card-actin R	CCT GAC TGG AAG GTA GAT GG		
29.	MSX-1-F	CCT TCC CTT TAA CCC TCA CAC	62 (°C)	287 bp
30.	MSX-1-R	CCG ATT TCT CTG CGC TTT TC		

31.	HNF3-F	GAC AAG TGA GAG AGC AAG TG	56 (°C)	237 bp
32.	HNF3-R	ACA GTA GTG GAA ACC GGA G		
33.	HNF4-F	TCT CAT GTT GAA GCC ACT GC	51 (°C)	501 bp
34.	HNF4-R	GGT TTG TTT CTC GGG TTG A		
35.	SOX17-F	ACG CCG AGT TGA GCA AGA	58 (°C)	82 bp
36.	SOX17-R	TCT GCC TCC TCC ACG AAG		
37.	FOXA2-F	GGG AGC GGT GAA GAT GGA	58 (°C)	92 bp
38.	FOXA2-R	TCA TGT TGC TCA CGG AGG AGT		
NCSC markers:				
39.	AP2-F	AAC ATG CTC CTG GCT ACA AAA	56 (°C)	71 bp
40.	AP2-R	AGG GGA GAT CGG TCC TGA		
41.	SOX9-F	GTA CCC GCA CTT GCA CAA C	56 (°C)	74 bp
42.	SOX9-R	TCT CGC TCT CGT TCA GAA GTC		
43.	p75-F	TCA TCC CTG TCT ATT GCT CCA	56 (°C)	99 bp
44.	p75-R	TGT TCT GCT TGC AGC TGT TC		
SMC markers:				
45.	VE-CADHERIN-F	GAA ACA GAG CCC AGG TCA TTA	59 (°C)	773 bp
46.	VE-CADHERIN-R	GAT GGT GAG GAT GCA GAG TAA G		
47.	αSMA-F	GAT CTG GCA CCA CTC TTT CTA C	59 (°C)	486 bp
48.	αSMA-R	CAG GCA ACT CGT AAC TCT TCT C		
49.	CALPONIN-F	ATG TCC TCT GCT CAC TTC AAC	59 (°C)	420 bp
50.	CALPONIN-R	CAC GTT CAC CTT GTT TCC TTT C		
51.	TRANSGELIN-F	GAA GAA AGC CCA GGA GCA TAA	59 (°C)	410 bp
52.	TRANSGELIN-R	CCA GGA TGA GAG GAA CAG TAG A		

Table S3: Primers for qPCR analysis. Summary of all qPCR primers used throughout this study. All primers were purchased from IDT®, Integrated DNA Technologies.

Specificity	Immunised animal	Clone	Staining dilution	Manufacturer, catalogue number
Primary antibody:				
Anti-α smooth muscle Actin (Alexa Fluor® 488)	Mouse	1A4	1:100	Abcam, ab184675
Anti-Peripherin	Rabbit	(Polyclonal)	1:50	MilliporeSigma, AB1530
Anti-β-Tubulin Isotype III	Mouse	SDL.3D10	1:50	MilliporeSigma, T5076
Secondary antibody:				
FITC Anti-rabbit	Goat	IgG	1:200	Abcam, ab97050
Alexa Fluor 647 Anti-mouse	Goat	IgG	1:200	Abcam, ab150115

Table S4: Antibodies used for ICC. Summary of all antibodies used throughout this study for ICC analysis.